

Equivalent Multilayer Bandwidth and Comparison between 13.4 nm and 14.4 nm for EUV Throughput Calculation

Weilun Chao^{1,2,*}, Eric Gullikson², and David Attwood^{1,2}

¹University of California at Berkeley, California

²Lawrence Berkeley National Laboratory, California

ABSTRACT

In the calculation of wafer throughput for EUV production tools, the multilayer mirrors are often approximated as a pass-band with a flat response equal to the highest reflectivity of the mirrors and a bandwidth equal to the FWHM of the reflectivity curve. However, the actual reflectivity response of the mirrors is an extended curve which peaks at wavelengths typically between 11-15 nm. With a broadband source, photons with wavelengths outside the FWHM of the mirror are also reflected, contributing to the throughput of the multimirror optical system. We present calculations to compare this simple model with the actual reflectivity curve for Mo/Si mirrors. The result shows that the model is a good approximation for throughput calculations.

In this paper, the optimal parameter values and center wavelengths for maximum throughput were also calculated for Mo/Si mirrors at different incidence angles and σ values. The simulation results confirm that for near-normal incidence, the optimal center wavelength for maximum integrated reflectivity is near 14.4 nm, in agreement with the previous work by R. Stuik et al.¹ As the off-normal incidence angle (ϕ) increases, the integrated reflectivity is reduced faster at longer wavelengths. The maximum integrated reflectivity centered at 13.4 nm is closer to that at the optimal center wavelengths for larger value of ϕ . The effect is more distinct for smaller σ . For ϕ equal to 15° (NA \sim 0.25) and peak reflectivity of 70%, the maximum integrated reflectivity of a 9-mirror optical system at 13.4 nm is only 2% less than that at 14.4 nm. If a 2-nm thick SiO₂ capping layer with roughness of 0.2 nm is included in the simulation, the optimal wavelength is unaffected and only the integrated reflectivity is reduced.

Keywords: Mo/Si, Multilayer, EUV Wavelengths, Reflectivity, Bandwidth, Throughput, Optimization, EUV lithography.

1. THROUGHPUT CORRECTION FACTOR

In designing an EUV lithography tool, one of the most important criteria to be met is wafer throughput. There are many factors that influence its value. In particular, the "transmission efficiency" of the multilayer mirrors in the system determines the amount of radiation from the light source that will expose the wafers. For a broadband source with a wavelength-independent intensity, the transmission efficiency is equal to the integrated area under the reflectivity curve of the mirror system (the integrated reflectivity). Often in wafer throughput calculations for EUV production tools, the multilayer mirrors are approximated as a pass-band with a flat response equal to the 9-mirror peak reflectivity ($(R_{pk})^9$) and a bandwidth equal to the Full Width at Half Maximum (FWHM) of the 9-mirror reflectivity curve (figure 1). The area of this rectangular pass band, which is the product of the $(R_{pk})^9$ and the FWHM, may not be the same as the integrated reflectivity (R_{int}). Thus, this pass-band model needs to be evaluated for accuracy.

Computer simulations using the multilayer program at our website² have been performed to calculate the integrated reflectivity for a 9-mirror system. An equivalent bandwidth, defined as the ratio of the integrated reflectivity to the 9-mirror peak reflectivity, was also calculated for different parameter sets. This bandwidth is the correct one to be used in the pass-band model. In the simulations, interface definition, including the effects of interdiffusion and roughness, are represented by a Debye-Waller factor σ . Γ is the ratio of the high Z material thickness to the bilayer period. λ_c is the center wavelength, defined as the mid-point of the line connecting the half maximum points of a reflectivity curve (figure 1). The incidence

* Correspondence: Email: wchao@lbl.gov; Telephone: 510-486-4079; Fax: 510-486-4550.

angle θ is measured from the surface, which is a common practice in the multilayer calculations due to the Bragg's law. For the convenience of readers from optics, we use the complementary angle ϕ , measured from the surface normal ($\phi = 90^\circ - \theta$).

Two σ values, 0.7 nm and 0.5 nm, are used in these simulations. The σ value of 0.7 nm was chosen by matching simulations with the nominal measured reflectivity. Figure 2 shows an experimental reflectivity curve for a single Mo/Si mirror along with a set of best-fitting parameters. Alternately, σ equal to 0.5 nm corresponds to the case where the peak reflectivity of a single mirror is around 70%, which is the goal for the EUV production tools.

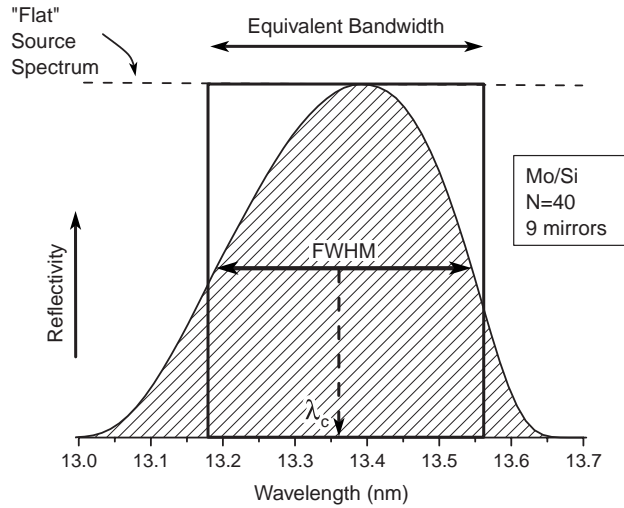


Figure 1. In a broadband source system with a wavelength independent intensity, the transmission efficiency of the multilayer mirrors is equal to the area under the reflectivity curve (the shaded area). Often in throughput calculations, this area is approximated by the area of a rectangle that has a height of the 9-mirror peak reflectivity ($(R_{pk})^9$) and a width of the FWHM of the 9-mirror reflectivity curve. As indicated in the diagram, the center wavelength, λ_c , is defined as the mid-point of the line connecting the half maximum points of the curve.

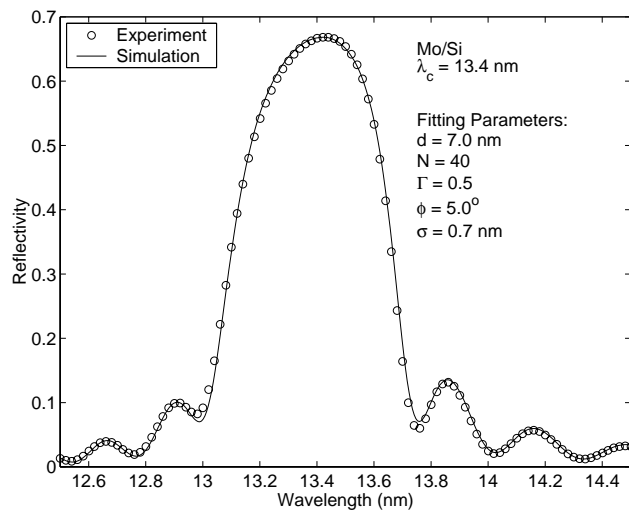


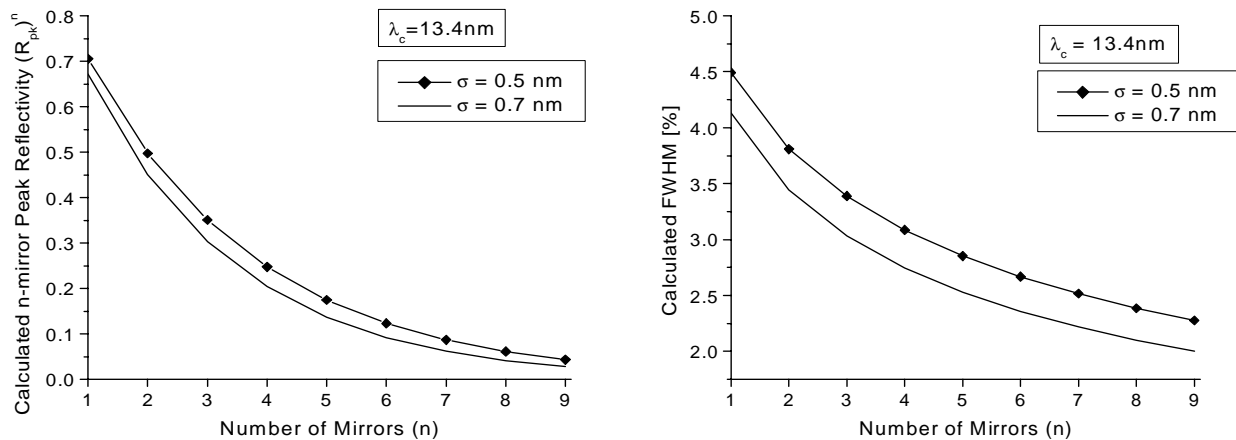
Figure 2. The measured reflectivity of a single Mo/Si mirror is plotted along with a simulation. The simulation clearly fits the measurement well. The interface definition parameter σ is a simple scalar quantity representing the effects of both material intermixing and roughness. The mirrors are fabricated using RF magnetron sputtering³. Courtesy of R. Soufli, Lawrence Livermore National Laboratory.

Mo/Si 9 Mirrors $\lambda_c = 13.4$ nm $d = 6.95$ nm $N = 40$ $\Gamma = 0.44$ $\phi = 5.0^\circ$ ($\theta = 85^\circ$)			
σ [nm]	FWHM [nm / %]	Equivalent Bandwidth [nm / %]	Throughput Correction Factor
0.5	0.306 / 2.28%	0.303 / 2.25%	0.990
0.7	0.269 / 2.00%	0.268 / 1.99%	0.996

Table 1. Calculations show that the FWHM is very close to the equivalent bandwidth, which is the correct bandwidth to be used in pass-band model. The throughput correction factor, which is the ratio of the equivalent bandwidth to the FWHM, is close to unity. ϕ and θ are measured from the normal and the surface, respectively.

σ [nm]	Throughput Correction Factor Mo/Si $d = 6.95$ nm $N = 40$ 9 Mirrors				
	$\Gamma = 0.40$ $\phi = 5.0^\circ$ ($\theta = 85^\circ$) $\lambda_c = 13.5$ nm	$\Gamma = 0.44$ $\phi = 5.0^\circ$ ($\theta = 85^\circ$) $\lambda_c = 13.4$ nm	$\Gamma = 0.48$ $\phi = 5.0^\circ$ ($\theta = 85^\circ$) $\lambda_c = 13.4$ nm	$\Gamma = 0.44$ $\phi = 10^\circ$ ($\theta = 80^\circ$) $\lambda_c = 13.3$ nm	$\Gamma = 0.44$ $\phi = 15^\circ$ ($\theta = 75^\circ$) $\lambda_c = 13.0$ nm
	0.5	0.991	0.990	0.992	0.991
0.7	0.999	0.996	1.00	1.00	0.999

Table 2. Throughput correction factors for different Γ , ϕ and σ values for a 9-mirror system. The results demonstrate that the equivalent bandwidth is approximated well by the FWHM for different parameter values.



1 Mirror $d = 6.95$ nm $N = 40$ $\Gamma = 0.44$ $\phi = 5.0^\circ$			
σ [nm]	R_{pk}	FWHM [nm / %]	Integrated Reflectivity [nm]
0.5	0.705	0.602 / 4.49%	0.490
0.7	0.672	0.554 / 4.13%	0.428

9 Mirrors $d = 6.95$ nm $N = 40$ $\Gamma = 0.44$ $\phi = 5.0^\circ$			
σ [nm]	$(R_{pk})^9$	FWHM [nm / %]	Integrated Reflectivity [nm]
0.5	0.0431	0.306 / 2.28%	0.0131
0.7	0.0278	0.269 / 2.00%	0.00745

Figure 3. Calculated n-mirror peak reflectivity and FWHM for mirrors with the parameters given in table 1 at 13.4nm. Their values and integrated reflectivity for 1 mirror and 9 mirrors are also tabulated. For a single mirror reflectivity of 70.5%, the calculated FWHM for a 9-mirror system is 2.28%.

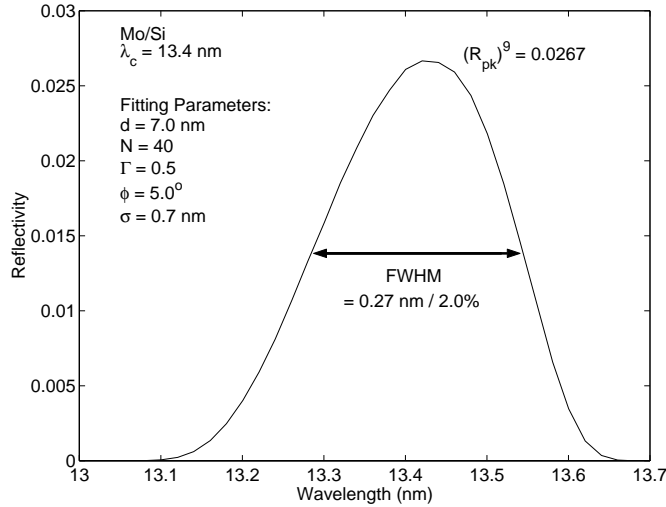


Figure 4. Shown is the 9th power of the measured reflectivity presented in figure 2. R_{pk} is the peak reflectivity of one mirror. The calculated FWHM of the 9-mirror reflectivity curve agrees with the FWHM of the 9th power of the measured reflectivity. Courtesy of R. Soufli, Lawrence Livermore National Laboratory.

The simulation results are presented in table 1. It is clear that the FWHM of the reflectivity curve agrees with the equivalent bandwidth to 2 significant figures. The throughput correction factor, which is the ratio of the equivalent bandwidth to the FWHM, is close to unity. This conclusion holds for different values of σ , Γ , and ϕ (table 2). Thus, in the case of a broadband source system, the FWHM for a 9-mirror system is a good approximation of the correct bandwidth for the pass-band model. Note that the simulation assumes that the nine mirrors have identical reflectivity profiles, which yields the highest transmission efficiency for a given parameter set. This assumption is reasonable based on recent measurements⁴.

In figure 3, the calculated n-mirror peak reflectivity and FWHM are shown as a function of the number of mirrors. Their values for one and nine mirrors are also tabulated. The result shows that for a single mirror reflectivity of 70.5%, the calculated FWHM for a 9-mirror system is 2.28%. For comparison, the 9th power of the measured reflectivity presented in figure 2 is plotted in figure 4. The calculated FWHM for a 9-mirror system agrees with the FWHM of the 9th power of the measured reflectivity curve.

2. OPTIMAL PARAMETERS FOR MAXIMUM THROUGHPUT

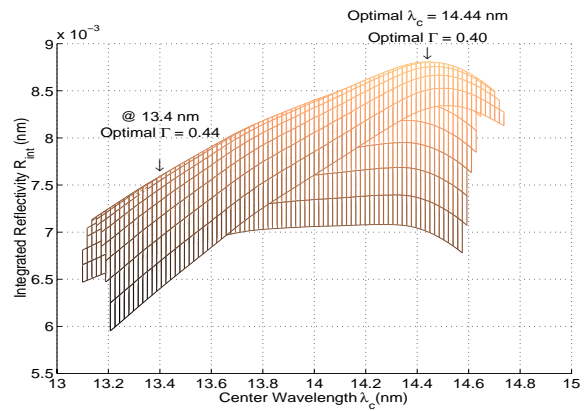
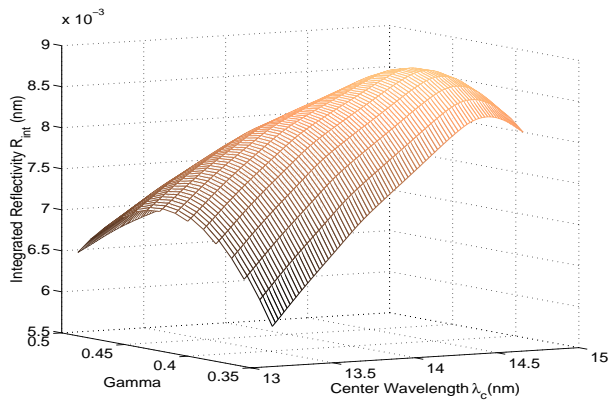
As discussed in section 1, the integrated reflectivity influences the wafer throughput of a system. It is important to optimize the multilayer mirror parameters for maximum integrated reflectivity.

The integrated reflectivity of a 9-mirror system was calculated with the simulation program for σ equal to 0.7 nm. Figure 5 shows the integrated reflectivity for a 9-identical-mirror system, as a function of Γ and λ_c , at different incidence angles. The optimal center wavelength for maximum integrated reflectivity is 14.4 nm, which agrees with the conclusion of R. Stuik et al.¹ The corresponding optimal Γ is 0.40. More interesting, as ϕ increases, the integrated reflectivity decreases faster at longer wavelengths. The variation of the integrated reflectivity for different λ_c is more gradual for larger off-normal angles of incidence. The relative maximum integrated reflectivity (κ_{int}), which is defined as:

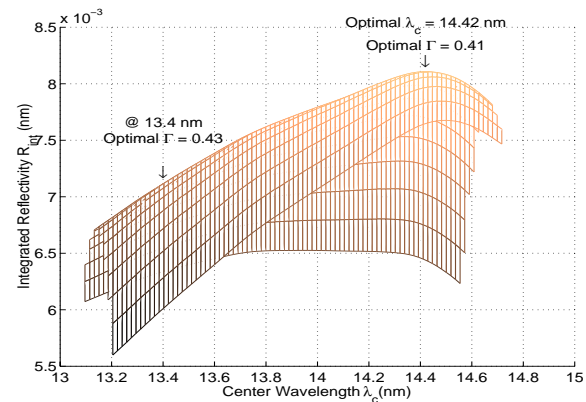
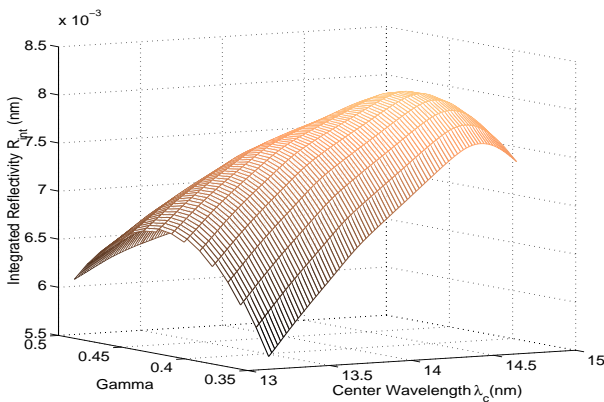
$$\kappa_{int} = \frac{\text{Maximum } R_{int} \text{ at } 13.4\text{nm}}{\text{Maximum } R_{int} \text{ at optimal center wavelength}} \quad (1)$$

is closer to unity at $\phi = 15^\circ$ (table 3).

$\sigma=0.7\text{nm}, \phi=0.0^\circ$



$\sigma=0.7\text{nm}, \phi=8.0^\circ$



$\sigma=0.7\text{nm}, \phi=15^\circ$

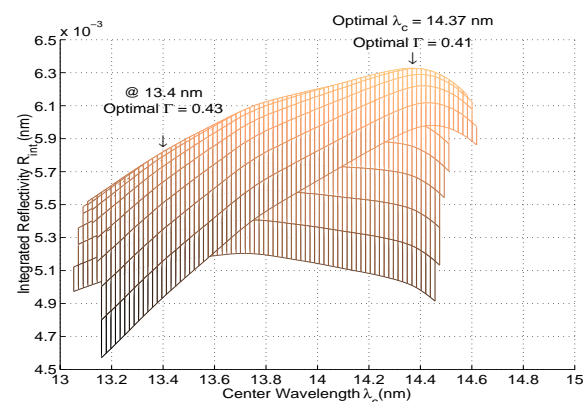
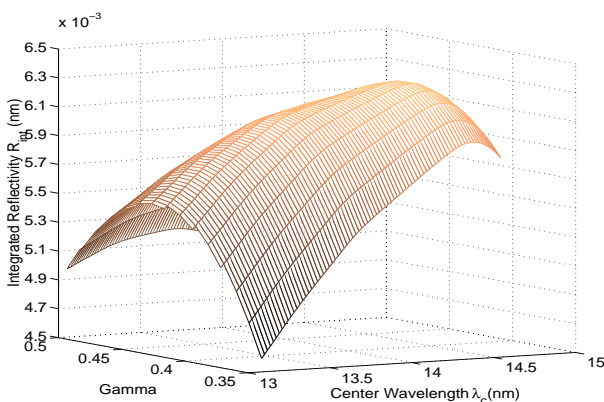
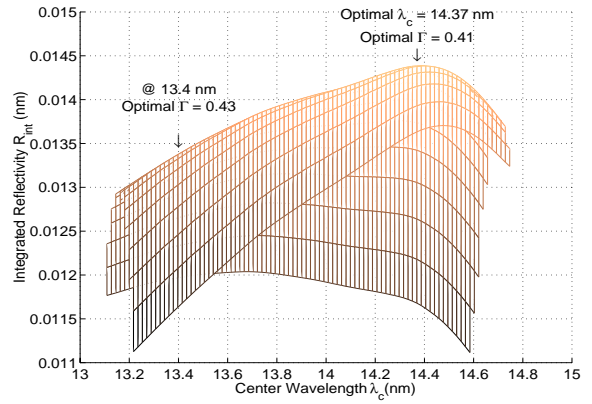
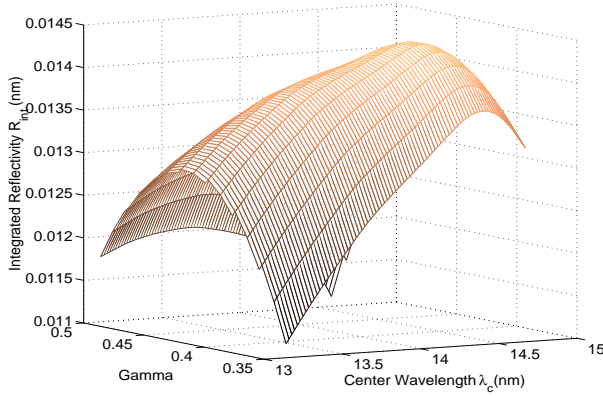
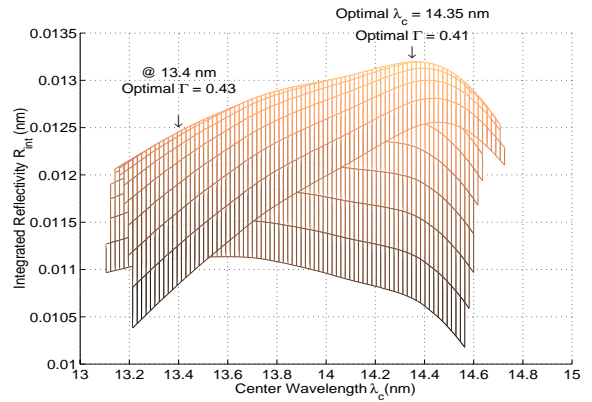
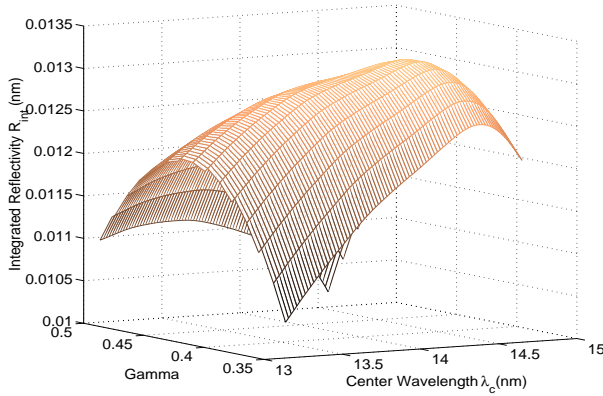


Figure 5. Shown in the left column is the integrated reflectivity of a 9-mirror system as a function of λ_c and Γ , with $\sigma = 0.7$ nm, at different incidence angles. R_{int} as a function of λ_c is plotted on the right hand side. The optimal center wavelength and Γ for maximum integrated reflectivity are 14.4 nm and 0.4 respectively. As ϕ increases (further off normal), the integrated reflectivity decreases faster at longer wavelengths. Thus, the slope of the crest of the integrated reflectivity curve is smaller for larger ϕ . This effect reduces the differences in maximum integrated reflectivity between 13.4 nm and 14.4 nm for larger off-axis angles.

$\sigma=0.5\text{nm}, \phi=0.0^\circ$



$\sigma=0.5\text{nm}, \phi=8.0^\circ$



$\sigma=0.5\text{nm}, \phi=15^\circ$

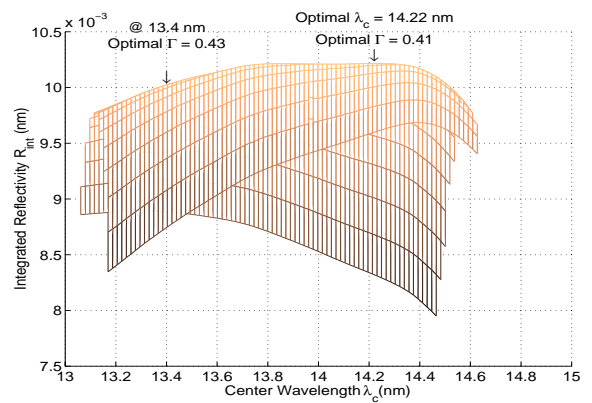
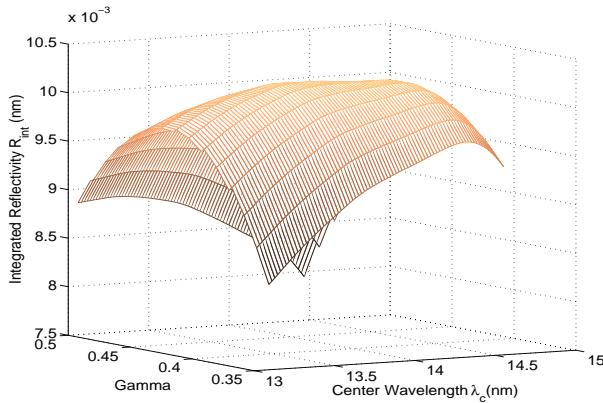


Figure 6. The integrated reflectivity of a 9-mirror system is calculated for a range of Γ and λ_c at three different angles with an interface parameter σ equal to 0.5 nm. As in the case of $\sigma = 0.7$ nm, the integrated reflectivity drops faster at longer wavelengths. However, the relative maximum integrated reflectivity κ_{int} is larger at the same angle for the smaller value of σ . At $\phi = 15^\circ$, the maximum integrated reflectivity at 13.4 nm is only 2% less than that at the optimal center wavelength.

		$R_{pk} @ 13.4 \text{ nm} = 67\%$ ($\sigma = 0.7 \text{ nm}$)			$R_{pk} @ 13.4 \text{ nm} = 70\%$ ($\sigma = 0.5 \text{ nm}$)		
		$\phi = 0.0^\circ$	$\phi = 8.0^\circ$	$\phi = 15^\circ$	$\phi = 0.0^\circ$	$\phi = 8.0^\circ$	$\phi = 15^\circ$
Optimal Center Wavelength	Max. R_{int} (nm)	0.00880	0.00811	0.00633	0.0144	0.0132	0.0102
	@ λ_c (nm)	14.44	14.42	14.37	14.37	14.35	14.22
	@ Γ	0.40	0.41	0.41	0.41	0.41	0.41
$\lambda_c = 13.4 \text{ nm}$	Max. R_{int} (nm)	0.00760	0.00712	0.00582	0.0134	0.0124	0.0100
	@ Γ	0.44	0.43	0.43	0.43	0.43	0.43
	κ_{int}	0.864	0.878	0.919	0.930	0.943	0.981

Table 3. The maximum integrated reflectivity at the optimal λ_c and Γ were calculated for Mo/Si mirrors at various angles, and for two σ values. Results at 13.4 nm are also shown. κ_{int} , which is proportional to the throughput at 13.4 nm relative to that at the optimal center wavelength, is also given. For the mirrors anticipated in the commercial production tools ($\sigma = 0.5$ nm case), the difference in throughputs between 13.4 nm and the optimal λ_c ranges from 2% to 7%. At 13.4 nm, the optimal Γ is at about 0.43 for all cases.

Similar simulations were also performed for $\sigma = 0.5$ nm. The integrated reflectivity at three different angles is shown in figure 6. Similar to the case of $\sigma = 0.7$ nm, as ϕ increases, the integrated reflectivity decreases faster at longer wavelengths. κ_{int} increases with the angle at about the same rate in this case as in the case for $\sigma = 0.7$ nm (table 3). However in this case, the value of κ_{int} is larger for all the angles; κ_{int} is above 0.9 for all the three angles. The maximum R_{int} centered at 13.4 nm is closer to that at the optimal center wavelength when σ decreases.

Table 3 summarizes the simulation results for the two cases. At 13.4 nm, the optimal Γ is about 0.43 for all cases. It is clear that for increasing ϕ , κ_{int} , which is proportional to the throughput at 13.4 nm relative to that at the optimal wavelength, increases. This effect is more pronounced for the smaller σ value. Looking to the future, anticipating mirrors with 70% reflectivity ($\sigma = 0.5$ nm case), we see that the difference in maximum integrated reflectivity between 13.4 nm and 14.4 nm ranges between 2% and 7%, for angles between 0° and 15° (NA ~ 0.25) off normal. Thus for a future 9-mirror optical system that covers angles in this range, the throughput difference at the two wavelengths is in the range of 4-5%.

The above simulations assume no capping layer on the multilayer mirrors. Further simulation using a more sophisticated program found that inclusion of a 2-nm thick SiO_2 capping layer with 0.2 nm roughness only decreases the integrated reflectivity, but does not vary the optimal Γ and the optimal center wavelengths. Therefore at 13.4 nm, Γ of 0.43 should still optimize the integrated reflectivity of a multimirror system with thin oxide layers developed on the surfaces.

3. CONCLUSION

For a 9-mirror system with a broadband, wavelength-independent intensity source,

- The 9-mirror FWHM is a good approximation to the equivalent bandwidth of the multimirror-system's pass-band model. This holds for different Γ , σ and ϕ values.
- The optimal Γ for maximum integrated reflectivity at 13.4 nm is 0.43 for different angles and σ values.
- For near normal incidence, the optimal center wavelength is around 14.4 nm, as reported by R. Stuijk et al.¹
- As the off-normal incidence angle ϕ increases, the throughput at 13.4 nm relative to that at 14.4 nm increases.
- The above point is particularly true for smaller σ . For mirrors with peak reflectivity of 70%, the throughput at 13.4 nm relative to that at 14.4 nm ranges from 2% to 7%, for angles from 0° to 15° (NA ~ 0.25).
- A 2-nm thick oxide layer on the surface was found to have negligible effect on optimal Γ and optimal center wavelengths, but only to decrease the integrated reflectivity.

The above findings may imply that production tools should be operated at around 14.4 nm for maximum throughput. In a system however, there are other important elements, which may degrade the system performance due to a longer operating wavelength. For instance, longer wavelengths would deteriorate resolution, due to its inversely proportional relationship to the wavelength. The conclusions obtained here should be considered along with all the other system constraints for optimal overall performance. In addition, note that κ_{int} is a relative quantity. Even though it is higher at larger off-normal angle, the normal incidence still yields the largest integrated reflectivity (absolute quantity) for all wavelengths. The method to achieve both large κ_{int} and large integrated reflectivity is to reduce the roughness and interdiffusion. For the small σ where $R_{\text{pk}} \sim 70\%$, and a 9-mirror, 0.25 NA optical system, these calculations show that the throughput at 13.4 nm is only about 4-5% less than that at 14.4 nm.

4. ACKNOWLEDGEMENTS

We would like to acknowledge Scott Hector for suggesting that we clarify this issue, Saša Bajt for the technical discussions, Regina Soufli and Eberhard Spiller (LLNL) for the multilayer data, and the generous support of the EUV Limited Liability Corporation and the Department of Energy's Office of Basic Energy Sciences.

5. REFERENCES

1. R. Stuik, E. Louis, A.E. Yakshin, P.C. Görts, E. L.G. Maas, R. Bijkerk, D. Schmitz, F. Scholze, G. Ulm, and M.Haidl, "Peak and integrated reflectivity, wavelength and gamma optimization of Mo/Si, and Mo/Be multilayer, multielement optics for extreme ultraviolet lithography," *J. Vac. Sci. Technol B*, **17**, 2998 (1999)
2. http://www-cxro.lbl.gov/optical_constants/multi2.html.
3. C. Montcalm, S. Bajt, P. B. Mirkarimi, E. Spiller, F. J. Weber, J. A. Folta, "Multilayer reflective coatings for extreme-ultraviolet lithography," *SPIE 3331*, 42(1998)
4. R. Soufli, E. Spiller, M. A. Schmidt, J. C. Davidson, R. F. Grabner, E. M. Gullikson, B. B. Kaufmann, S. L. Baker, H. N. Chapman, R. M. Hudyman, J. S. Taylor, C. C. Walton, C. Montcalm, J. A. Folta, "Multilayer optics for an extreme ultraviolet lithography tool with 70 nm resolution," *SPIE 4343*, (2001)